applied sciences

MDPI

Article

Major Depressive Disorder and Oxidative Stress: In Silico Investigation of Fluoxetine Activity against ROS

Cecilia Muraro [1], Marco Dalla Tiezza [1], Chiara Pavan [2], Giovanni Ribaudo [3], Giuseppe Zagotto [4] and Laura Orian [1,*]

1 Department of Chemical Sciences, University of Padova, Via Marzolo 1, 35131 Padova, Italy
2 Department of Medicine, University of Padova, Via Giustiniani 2, 35128 Padova, Italy
3 Department of Molecular and Translational Medicine, University of Brescia, Viale Europa 11, 25123 Brescia, Italy
4 Department of Pharmacological Sciences, University of Padova, Via Marzolo 5, 35131 Padova, Italy
* Correspondence: laura.orian@unipd.it; Tel.: +39-049-8275140

Received: 5 August 2019; Accepted: 23 August 2019; Published: 3 September 2019

Featured Application: Due to the seriousness of depressive disorders and their social implications, any strategy to improve clinical symptoms are of considerable importance. It is recognized that oxidative stress negatively impacts on this and other psychiatric diseases. Fluoxetine, a well-known and largely prescribed antidepressant drug, has antioxidant capacity, but, based on our analysis, this is due to its efficiency in increasing the concentration of free serotonin, rather than its direct ROS scavenging activity.

Abstract: Major depressive disorder is a psychiatric disease having approximately a 20% lifetime prevalence in adults in the United States (U.S.), as reported by Hasin et al. in *JAMA Psichiatry* 2018 *75*, 336–346. Symptoms include low mood, anhedonia, decreased energy, alteration in appetite and weight, irritability, sleep disturbances, and cognitive deficits. Comorbidity is frequent, and patients show decreased social functioning and a high mortality rate. Environmental and genetic factors favor the development of depression, but the mechanisms by which stress negatively impacts on the brain are still not fully understood. Several recent works, mainly published during the last five years, aim at investigating the correlation between treatment with fluoxetine, a non-tricyclic antidepressant drug, and the amelioration of oxidative stress. In this work, the antioxidant activity of fluoxetine was investigated using a computational protocol based on the density functional theory approach. Particularly, the scavenging of five radicals ($HO^{\bullet}$, $HOO^{\bullet}$, $CH_3OO^{\bullet}$, $CH_2{=}CHOO^{\bullet}$, and $CH_3O^{\bullet}$) was considered, focusing on hydrogen atom transfer (HAT) and radical adduct formation (RAF) mechanisms. Thermodynamic as well as kinetic aspects are discussed, and, for completeness, two metabolites of fluoxetine and serotonin, whose extracellular concentration is enhanced by fluoxetine, are included in our analysis. Indeed, fluoxetine may act as a radical scavenger, and exhibits selectivity for $HO^{\bullet}$ and $CH_3O^{\bullet}$, but is inefficient toward peroxyl radicals. In contrast, the radical scavenging efficiency of serotonin, which has been demonstrated in vitro, is significant, and this supports the idea of an indirect antioxidant efficiency of fluoxetine.

Keywords: free radical scavengers; antioxidants; fluoxetine; depressive disorder; major; oxidative stress; DFT calculations; reactive oxygen species

1. Introduction

1.1. Background

Fluoxetine hydrochloride (3-(p-trifluoromethylphenoxy)-N-methyl-3-phenylpropylamine HCl) (**1**, Figure 1) was presented to the community of physicians and medicinal chemists in the early 1970s, when it was described in a scientific journal as a selective serotonin-reuptake inhibitor [1]. Nevertheless, several years were required to fully develop this compound, which was later approved for the treatment of depression by the Food and Drug Administration (FDA, 1987) and marketed as Prozac (Eli Lilly) [2]. Fluoxetine is the prototype of selective serotonin-reuptake inhibitors (SSRIs), the first member of a new class of antidepressants initially introduced in the United States (U.S.) [2]. Moreover, it was also the first SSRI made available for clinical use in most countries besides the U.S. [3]. Despite early skepticism, Prozac became a true symbol of successful "blockbuster" drugs through the years. In fact, a fluoxetine capsule was depicted in the cover of *Newsweek*, celebrated as "a breakthrough drug for depression" by the same magazine (1990), as one of the "Pharmaceutical Products of the Century" by Fortune (1999) and, more in general, as the "happiness pill" in the pop culture [2].

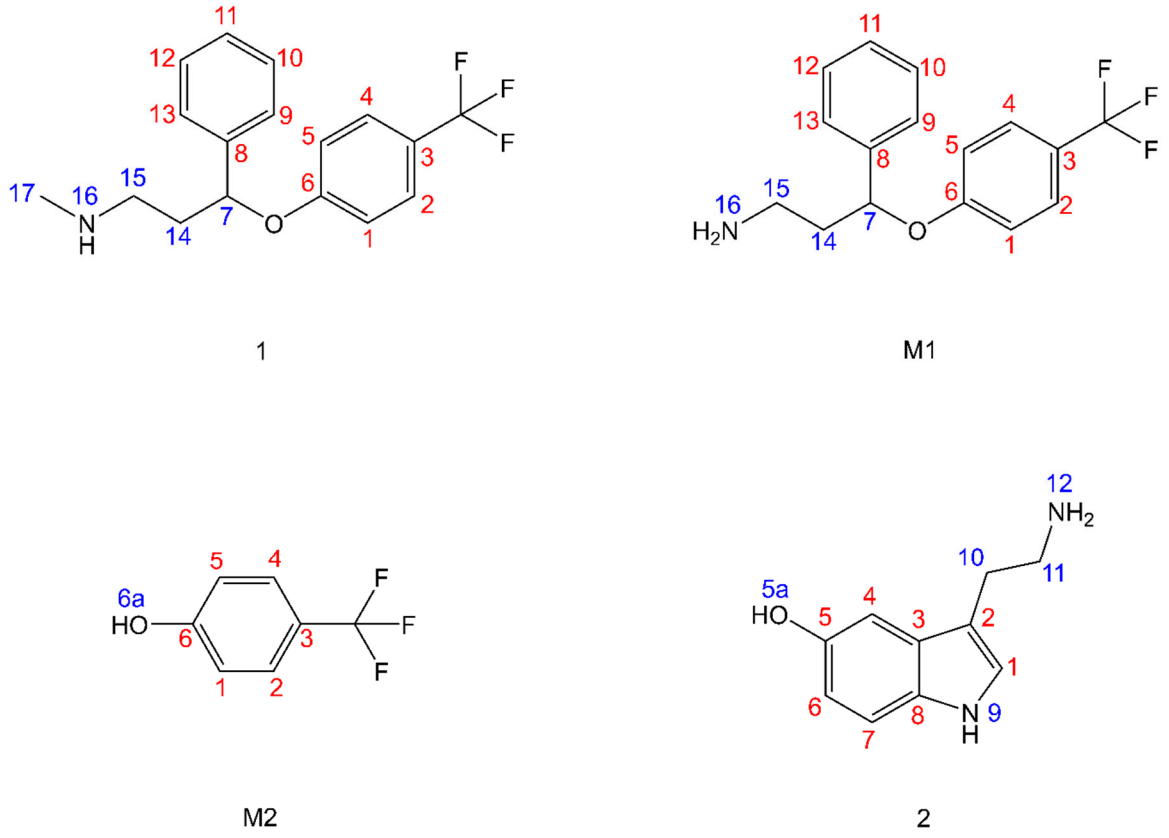

Figure 1. Fluoxetine (**1**) and its metabolites (**M1** and **M2**); serotonin (**2**).

By blocking the reuptake of serotonin (**2**, Figure 1) binding the neuronal presynaptic serotonin transporter SLC6A4 (Solute Carrier Family 6 Member 4), fluoxetine promotes an increase of the concentration of the neurotransmitter in the synaptic cleft. This leads to enhanced postsynaptic neuronal activity of the serotoninergic neurotransmission with limited effects on catecholaminergic neurons, differently from tricyclic antidepressants (TCAs) [4–6]. The observed therapeutic results are mainly due to the effect on the 5-HT_{2C} receptors [7].

Fluoxetine is structurally related to diphenhydramine, which is an antihistaminic that had been developed 30 years before [5]. It is a racemic mixture of two enantiomers, R(−)-fluoxetine and S(+)-fluoxetine, the latter being 1.5 times more potent in inhibiting serotonin reuptake [3,8].

The molecular basis and the binding mode justifying this difference were studied from a structural point of view [9]. After the patent on racemic fluoxetine expired, attempts to develop S(+)-fluoxetine formulations were pursued [10]. Fluoxetine has been marketed in capsules (the typical dose is 20 mg for the treatment of depression), but formulations for prolonged drug release were also studied [5,11]. It has been approved worldwide for the treatment of major depression, but it is also effective against several other syndromes [1,5], with a clinical efficacy similar to that of TCAs and fewer cardiovascular and anticholinergic side effects [5]. Fluoxetine effectively acts on a wide spectrum of mood disorders and protects against the adverse effects of different types of stressors by decreasing some effects of stress on the immune system and by protecting against oxidative damage. Different molecular mechanisms have been proposed to explain its neuroprotective effects, including BDNF (Brain-derived Neurotrophic Factor) release, antagonism on NMDA (N-methyl-D-aspartate) receptors, the inhibition of NF-kB (Nuclear Factor Kappa B Subunit 1) activity, and inhibition of the release of pro-inflammatory factors (TNF-α, Tumor Necrosis Factor-Alpha, IL-1β, Interleukin 1 Beta) from microglial cells [12]. However, the underlying mechanisms of its therapeutic efficacy remain unclear, particularly those related to its antioxidant activity. The brain is very susceptible to oxidative stress, since it has a high energy requirement, and oxidative stress has been implicated in the pathogenesis of many psychiatric and degenerative disorders. Moreover, aversive stimuli promote peripheral oxidative stress, which leads to an increase in the generation of reactive oxygen species (ROS) in peripheral blood lymphocytes, granulocytes, and monocytes, and a meta-analysis showed an increase in oxidative stress markers such as 8-oxo-2′deoxyguanosine and F2-isoprostanes in depressed patients [13]. High level of proteins and lipid peroxidation and an imbalance between superoxide dismutase and catalase were found in the brain and in the submitochondrial particles into the brain, and the antidepressant treatment improves these oxidative stress parameters in patients with depression [14]. Higher serum total oxidant status and a lower serum total antioxidant capacity in depressed patients were reversed after treatment with antidepressants in animal models of depression as well as in patients [15–17].

It has been postulated that the capacity of fluoxetine to ameliorate the oxidative stress damage may be either due to a direct role of the molecule or achieved through the stimulation of some antioxidant enzymes. Oxidative stress can damage the cell through lipid peroxidation, DNA or protein oxidation, and mitochondrial damage [18]. In this connection, it must be pointed out that the central nervous system is composed of a high percentage of phospholipids, which can undergo peroxidation and generate ROS, and may eventually lead to potentially harmful conditions for cellular structures [19]. It has been demonstrated, mainly in preclinical but also in clinical studies, that fluoxetine provides a beneficial antioxidant effect through a combination of mechanisms: the inhibition of lipid peroxidation, an increase of glutaminergic transmission, the restoration of the normal metabolism of monoamines, the influence on ion balance, and a reduction of inflammation, which is connected to ROS production [18,20,21]. Kolla et al. showed that amitriptyline and fluoxetine protect against oxidative stress-induced damage in rat pheochromocytoma (PC12) cells, contrasting the effects of H_2O_2 [22]. Caiaffo et al. recently reviewed the evidences of the anti-inflammatory, antiapoptotic, and antioxidant activity of fluoxetine [19]. Particularly, several contributions highlighted that fluoxetine may positively influence, to different degrees, the expression and functioning of "endogenous components of the antioxidant defense system" (superoxide dismutase (SOD), catalase (CAT), glutathione peroxidase (GPx) as well as "non-enzymatic antioxidant components". Moreover, the same authors suggested that, based on the reported findings, fluoxetine provides its antioxidant effect only under conditions of oxidative damage, which can be connected to other diseases (diabetes, depression, ischemia) and/or polypharmacological treatments [19,23]. It must be also pointed out that very recently, Dalmizrak et al. studied the inhibitory potential of fluoxetine on glutathione reductase activity [24].

Kalogiannis et al. investigated the role of fluoxetine in ameliorating the condition of a mice model of cerebral inflammation. According to the working hypothesis of the authors, this SSRI may enhance the cerebral antioxidant capacity of serotonin by increasing its extracellular concentration in the brain [25]. In fact, serotonin is known to possess antioxidant capacity, and has been previously

studied in silico as well as in vitro for its potentially protective role for the cell [26,27]. At the same time, the connection between the levels of this neurotransmitter and the antioxidant defense has been clearly established [28], and evidences of the in vitro antioxidant and radical scavenging properties of serotonin have been demonstrated using a combination of experimental techniques [29].

1.2. Aim of This Work

Computational methodologies are nowadays largely employed to rationalize chemical and biochemical phenomena. Particularly, accurate mechanistic studies on the control of oxidative stress by endogenous defenses, including enzymes such as glutathione peroxidase [30–32], and molecular drugs that act as mimics of these enzymes [33–37] or as radical scavengers [38] have been reported by some of us. In this work, we investigate in silico the antioxidant activity of fluoxetine via HAT (hydrogen atom transfer) and RAF (radical adduct formation) mechanisms. The purpose is to assess its radical scavenging efficiency; for completeness, two metabolites of fluoxetine (**M1** and **M2**, Figure 1) are included. Finally, the analysis is performed also on serotonin, the extracellular concentration of which is enhanced in patients treated with fluoxetine.

2. Materials and Methods

2.1. Calculation of $\Delta G^{\circ}_{HAT/RAF}$

A conformational analysis of **1** was carried out using the semi-empirical quantum mechanical method GFN2-xTB [39–41]. Conversely, the most stable conformer of **2** was taken from [27]. For all the studied reactions of HAT and RAF, geometry optimizations of the reactants and products were performed in the gas phase without any constraint, using the M06-2X functional [42] combined with the 6-31G(d) basis set, as implemented in Gaussian 16 [43]. Spin contamination was checked for the doublet ground state species to assess the reliability of the wavefunction. Frequency calculations were carried out at the same level of theory (M06-2X/6-31G(d)) in order to confirm the stationary points (all positive frequencies) and to obtain the thermodynamic corrections at 1 atm and 298 K. Afterwards, single-point energy calculations were performed at M06-2X/6-311+G(d,p) in the gas phase in order to obtain more accurate energy values, and subsequently, at the same level of theory, in benzene and water using the continuum Solvation Model based on Density (SMD) [44,45]. This level of theory is denoted in the text (SMD)-M06-2X/6-311+G(d,p)//M06-2X/6-31G(d,p). Benzene and water mimic an apolar and a polar environment, respectively [46]. The calculation of the HAT/RAF Gibbs free energies for all the available sites was streamlined using an in-house Python script.

Natural spin densities and atomic charges were calculated with the natural population analysis (NPA) for C4 sites in 1 and its metabolites (Scheme 3) [47]. The electron spin density surfaces related to the localized natural bond orbitals (NBO) were also drawn for selected structures with Multiwfn [48] with a high-quality grid and the isodensity value of 0.003.

2.2. Calculation of $\Delta G^{\ddagger}_{HAT}$

On the basis of ΔG°_{HAT}, the most reactive sites were identified, and the energy barriers were computed (level of theory: (SMD)-M06-2X/6-311+G(d,p)//M06-2X/6-31G(d,p)). The single imaginary frequency of all the transition states was analyzed to ensure that it corresponded to the correct vibrational mode. In gas phase, a reactant complex (RC) and a product complex (PC) exist on the potential energy surface, before and after the transition state (TS), respectively. In all cases, these species are located at higher energy than the free reactants and products; thus, energy barriers were calculated, referring to the free reactants in the gas phase as well as in the solvent [49].

3. Results

Radical scavenging occurs via different mechanisms, among which hydrogen atom transfer (HAT) and radical adduct formation (RAF) have been identified as mostly efficient in several organic

molecules displaying antioxidant properties, including Trolox [50], melatonin [51], and capsaicin [52], but also psychotropic drugs such as zolpidem [38]. These mechanisms are summarized in Figure 2.

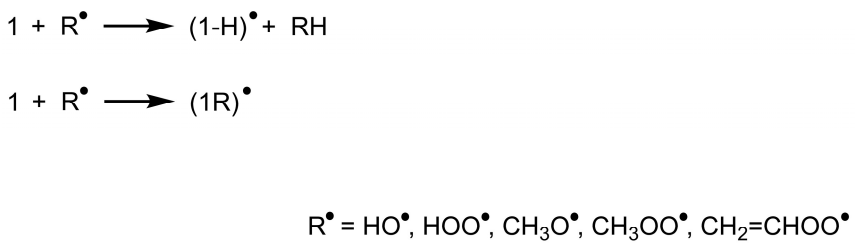

Figure 2. Hydrogen atom transfer (HAT) and radical adduct formation (RAF) in fluoxetine (**1**).

HAT implies the transfer of H• from one site of the scavenger to the ROS. Conversely, RAF consists in the addition of the ROS to a double bond site. The calculations of $\Delta G^{\circ}_{HAT/RAF}$ have been streamlined using an in-house Python script, in order to automatically screen all the available sites of fluoxetine (**1**), its metabolites, and serotonin (**2**). Activation energies $\Delta G^{\ddagger}_{HAT/RAF}$ were computed only for the most exergonic reactions. HAT results are presented in the following subsections, while the RAF mechanism and the related energetics are included in the Discussion.

3.1. Fluoxetine

HAT Gibbs free energy (ΔG°_{HAT}) was computed for all the possible sites of fluoxetine (Figure 1) considering five ROSs, i.e., HO•, HOO•, $CH_3OO^{\bullet}$, CH_2=CHOO•, and $CH_3O^{\bullet}$ (Figure 2). The results are shown in Figure 3 and reported in Table S1. HO• is the most reactive and electrophilic oxygen-centered radical; the peroxyl radicals HOO• and $CH_3OO^{\bullet}$ are much less reactive, and thus can reach remote cellular locations; CH_2=CHOO• was chosen to mimic larger unsaturated peroxyl radicals; finally, $CH_3O^{\bullet}$ has an intermediate reactivity between HO• and the peroxyl radicals.

The thermodynamic results, i.e., reaction energies are discussed first. Referring to the gas-phase values, it emerges that fluoxetine is selective for HO• and alkoxyl radicals, excluding—in this latter case—the sites on the phenyl rings; it is not selective for peroxyl radicals. Focusing on the scavenging of HO•, HAT is thermodynamically strongly favored from N site 16 and from C sites 7, 14–15 and 17, among which 7 and 15 are associated to the largest (negative) values, i.e., −26.06 and −26.88 kcal mol^{-1}. A similar ΔG°_{HAT} is computed for HAT from N site 16 (−24.24 kcal mol^{-1}) and from C site 17 (−24.87 kcal mol^{-1}). In solvent, the same trends are maintained, the ΔG°_{HAT} becoming more negative with increasing polarity, and the largest negative value is found for HAT from N 16 in water (−31.41 kcal mol^{-1}). When considering $CH_3O^{\bullet}$, in the gas phase, HAT is thermodynamically favored only from sites 7 and 14–17. Meanwhile, ΔG°_{HAT} values are approximately half (in absolute value) those computed for HO•, except for those associated to C 14 and N 16, which are drastically reduced, changing from −18.31 and −24.24 kcal mol^{-1} to −3.81 and −9.73 kcal mol^{-1}, respectively. Also, for $CH_3O^{\bullet}$, increasing the solvent polarity results in thermodynamically more favored reactions. The reactivity of C sites 14 and 15 of fluoxetine recalls the reactivity of the topologically similar C site 4 in melatonin [46] and zolpidem [38]. By comparing the transfer of the methylene hydrogens to HO• in these compounds, which were computed at the same level of theory, [38] the order is zolpidem (−33.3 kcal mol^{-1}) > melatonin (−28.9 kcal mol^{-1}) > fluoxetine (−26.88 kcal mol^{-1}). The value of ΔG°_{HAT} involving HO• of Trolox is −38.7 kcal mol^{-1} [38]. As mentioned above, fluoxetine is not selective for peroxyl radicals: a negative value of ΔG°_{HAT}, i.e., −1.23 kcal mol^{-1}, is computed only for CH_2=CHOO• in water.

The transition states and thus the activation energies were computed only for the exergonic reactions; they are reported in Table 1.

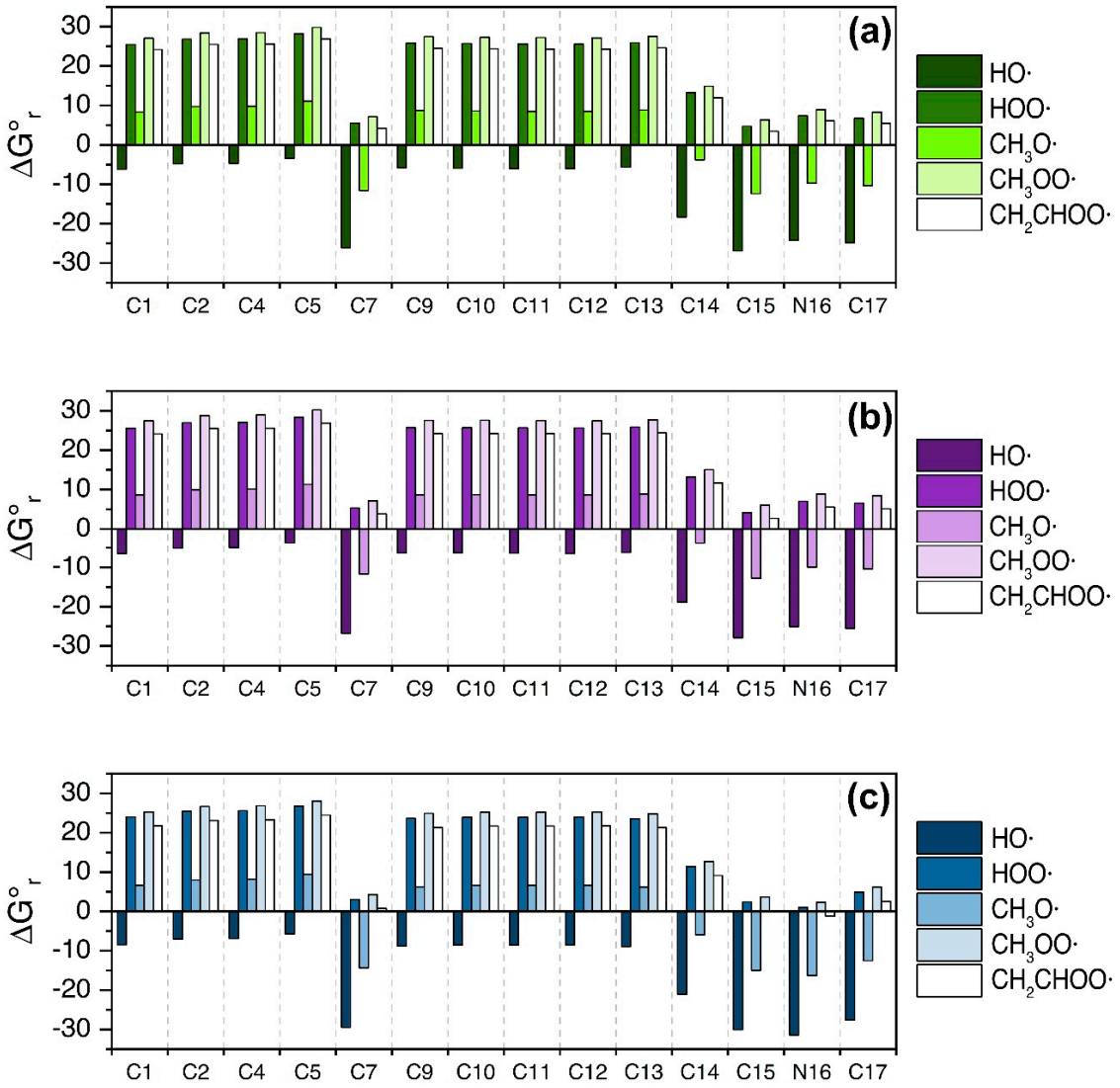

Figure 3. ΔG°_{HAT} (kcal mol^{-1}) in the gas phase (**a**), in benzene (**b**), and in water (**c**) for the scavenging of HO$^{\bullet}$, $CH_3O^{\bullet}$, HOO$^{\bullet}$, $CH_3OO^{\bullet}$, and CH_2=CHOO$^{\bullet}$ through HAT from all the available sites of **1**. Level of theory: (SMD)-M06-2X/6-311+G(d,p)//M06-2X/6-31G(d).

Table 1. $\Delta G^{\ddagger}_{HAT}$ (kcal mol^{-1}) in the gas phase, benzene, and water, for the scavenging of HO$^{\bullet}$ and $CH_3O^{\bullet}$ through HAT in **1**. Level of theory: (SMD)-M06-2X/6-311+G(d,p)//M06-2X/6-31G(d).

Site	Gas Phase	Benzene	Water	Gas Phase	Benzene	Water
		HO$^{\bullet}$			$CH_3O^{\bullet}$	
7	6.57	8.58	10.03	13.69	16.07	16.45
14	7.48	8.91	9.54	14.95	16.72	16.26
15	5.39	5.95	4.24	11.67	12.35	9.74
16	3.68	4.01	0.85	8.34	9.01	6.18
17	7.84	8.35	5.50	14.43	15.28	12.19

Considering the HAT from C sites 7 and 14, the energy barriers increase almost in all cases when going from the gas phase to benzene and water. Conversely, for the HAT from C sites 15 and 17 and N site 16, the lowest activation energies are computed in water. Kinetically, the easiest scavenging involves HO$^{\bullet}$ in water from N 16, which is also the most thermodynamically favored reaction.

3.2. Fluoxetine Metabolites

The pharmacokinetic and metabolic aspects of fluoxetine in the human body have been described in detail by Hiemke and Hartter and by Mandrioli et al. [3,5]. Fluoxetine is a lipophilic molecule that is almost completely absorbed after oral administration. Oral bioavailability is lower than 90% of the dose, due to hepatic first-pass extraction [53]. Fluoxetine highly accumulates in lungs, mainly due to lysosomal trapping, and it is characterized by a large volume of distribution (Vd), similar to that of TCAs [3]. Accumulation in the brain is lower than that of other SSRIs, with a brain to plasma ratio of 2.6:1 compared with 24:1 for fluvoxamine [54]. Fluoxetine is also characterized by a long half-life ($t_{1/2}$), ranging from 24 h to 4 days, which implies that between 1–22 months may be required to reach steady-state conditions during therapy [3,8]. Moreover, it has been observed that fluoxetine follows non-linear kinetics, since there is a disproportion between increase in blood concentration after dose escalation [3]. With a 20–60 mg/die dose, plasma levels range from 50 to 480 ng/mL [5].

R(−)-fluoxetine and S(+)-fluoxetine have different metabolic rates, since a four times greater clearance has been reported for the first, which means that the $t_{1/2}$ of the more active S(+) enantiomer is shorter [4]. Hepatic cytocrome P450 enzymes are responsible for the biotransformation in humans. Particularly, fluoxetine undergoes metabolic transformation mediated by CYP isoenzymes, and less than 10% is excreted unchanged or as fluoxetine N-glucuronide [55]. CYP2D6, and other isoforms such as CYP2C9 and CYP3A4, mediate N-demethylation to the active metabolite norfluoxetine (**M1**). Concerning this metabolite, the pharmacological difference between enantiomers is even stronger: S(+)-norfluoxetine is 20 times more potent in inhibiting serotonin uptake than the R(−) isomer [3]. Norfluoxetine has a longer $t_{1/2}$ (4–16 days), and it can also be converted to its glucuronide form [3,5]. CYP2D6 also mediates the further degradation of R(−)-fluoxetine, S(+)-fluoxetine, and S(+)-norfluoxetine, without influencing R(−)-norfluoxetine concentration. Other studies report that CYP2C9 is more selective for the R(−) enantiomer, while the remaining isoforms catalyze N-demethylation on both isomers with similar rates [56]. The oxidative O-dealkylation reaction of fluoxetine can also lead to the formation of another metabolite, p-trifluoromethylphenol (**M2**). This reaction is mediated by CYP2C19 and CYP3A4 [5].

Several analytical methods have been developed through the years for the identification and quantification of fluoxetine and its metabolites in biological samples. HPLC-UV, mass spectrometry, and gas chromatography are some of the tools included in the methods currently available in the literature [5,57–59]. The choice of applying one or more of such analytical techniques should also take into consideration the stereochemical aspects [6]. For the sake of completeness, we have investigated the scavenging activity of **M1** and **M2**.

ΔG°_{HAT} are shown in Figure 4 and reported in Table S2.

The results of norfluoxetine are very similar to those of **1**. Scavenging via HAT is thermodynamically most favored from C sites 7, 14–16. Particularly, in the gas phase, the largest (negative) ΔG°_{HAT} values are found for C 7 (−30.94 and −16.43 kcal mol^{-1} for HO$^{\bullet}$ and $CH_3O^{\bullet}$), which become even more negative with increasing solvent polarity, i.e., −31.48 and −16.41 kcal mol^{-1} in benzene and −32.61 and −17.53 kcal mol^{-1} in water, respectively. In general, the reactivity of **M1** from these sites toward the hydroxyl and methoxyl radicals via HAT is enhanced when compared to that of **1**. Particularly, focusing on site C 7, negative values of ΔG°_{HAT} are computed also for CH_2=CHOO$^{\bullet}$, ranging from −0.64 kcal mol^{-1} in the gas phase to −0.90 and −2.44 kcal mol^{-1} in benzene and water, respectively. The activation energies, which were computed for the exergonic reactions, are reported in Table 2.

When considering **M2**, the only strongly reactive site via HAT is 6a, i.e., the alcohol functional group. The selectivity is limited to the HO$^{\bullet}$ and $CH_3O^{\bullet}$. ΔG°_{HAT} values range from −11.24 kcal mol^{-1} for the alkoxyl radical in the gas phase to −27.09 kcal mol^{-1} for the hydroxyl radical in water. The activation energies increase with solvent polarity and are higher for this latter radical, with a value of 12.40 kcal mol^{-1} in water to be compared with 5.38 kcal mol^{-1} computed for the alkoxyl radical in the same conditions.

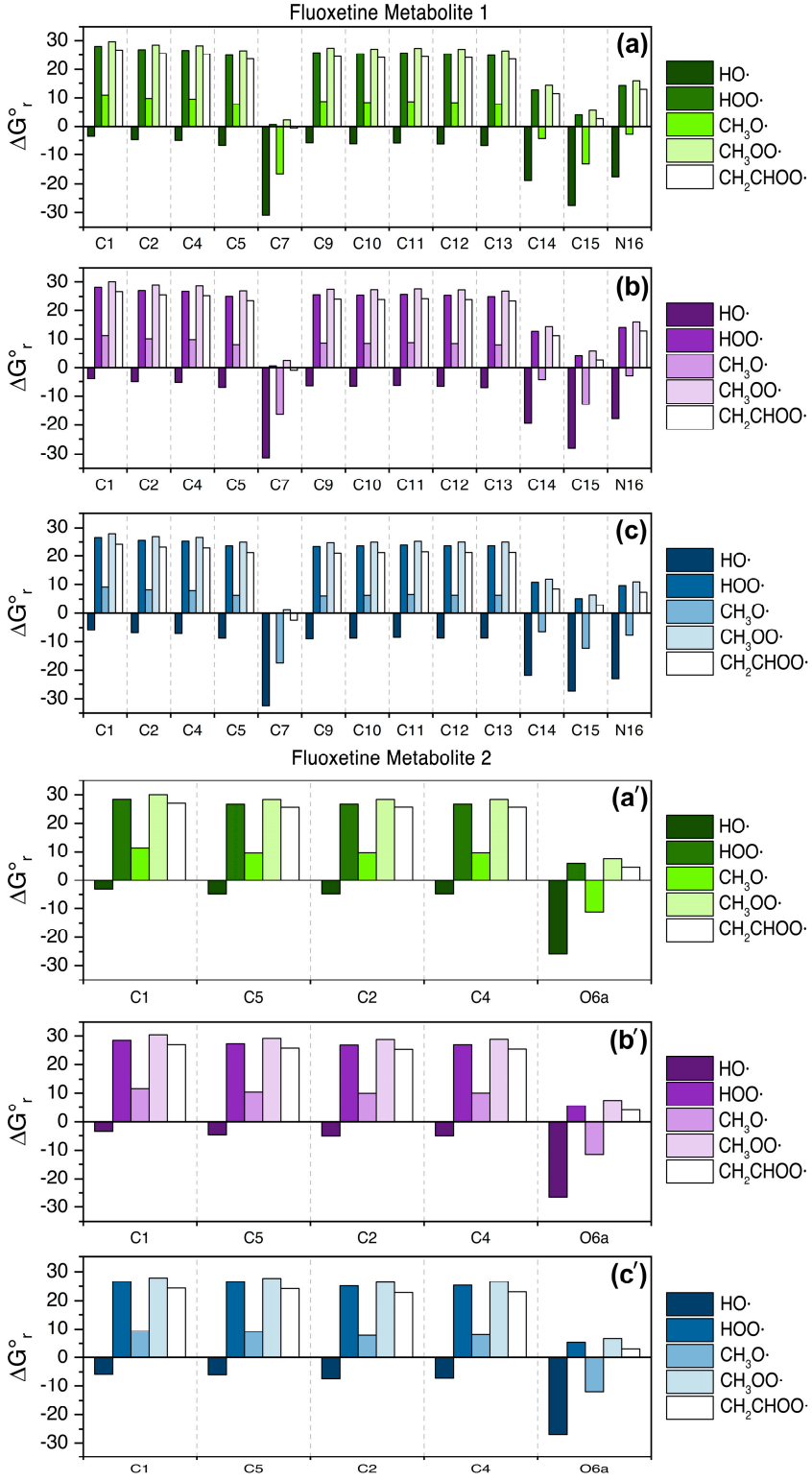

Figure 4. ΔG°_{HAT} (kcal mol^{-1}) in gas-phase for fluoxetine metabolite 1 (**a**) and fluoxetine metabolite 2 (**a′**), in benzene for fluoxetine metabolite 1 (**b**) and fluoxetine metabolite 2 (**b′**), and in water for fluoxetine metabolite 1 (**c**) and fluoxetine metabolite 2 (**c′**) for the scavenging of HO$^{\bullet}$, $CH_3O^{\bullet}$, HOO$^{\bullet}$, $CH_3OO^{\bullet}$, and CH_2=CHOO$^{\bullet}$ through HAT from all the available sites of fluoxetine metabolite 1 (**M1**) and metabolite 2 (**M2**). Level of theory: (SMD)-M06-2X/6-311+G(d, p)//M06-2X/6-31G(d).

Table 2. $\Delta G^{\ddagger}_{HAT}$ (kcal mol^{-1}) in the gas phase, benzene, and water, for the scavenging of HO$^{\bullet}$ and $CH_3O^{\bullet}$ through HAT in **M1** and **M2**. Level of theory: (SMD)-M06-2X/6-311+G(d,p)//M06-2X/6-31G(d).

Site	Gas Phase	Benzene	Water	Gas Phase	Benzene	Water
		HO$^{\bullet}$			$CH_3O^{\bullet}$	
7	5.40	7.99	11.58	12.23	15.19	17.63
14	5.36	7.33	10.44	13.64	15.96	18.05
15	4.35	5.42	6.69	9.79	11.07	11.55
16	3.84	4.87	5.71	11.37	12.61	13.07
6a [1]	6.21	8.26	12.40	1.83	3.11	5.38

[1] This is the only strongly reactive site (large negative ΔG°_{HAT}) of **M2** toward both HO$^{\bullet}$ and $CH_3O^{\bullet}$.

3.3. Serotonin

The radical scavenging activity of serotonin (**2**) was also systematically investigated, and the results are shown in Figure 5 and Table S3. The scavenging activity of **2** was expected for its well-known antioxidant capacity, which was likely related to its structural similarity to melatonin.

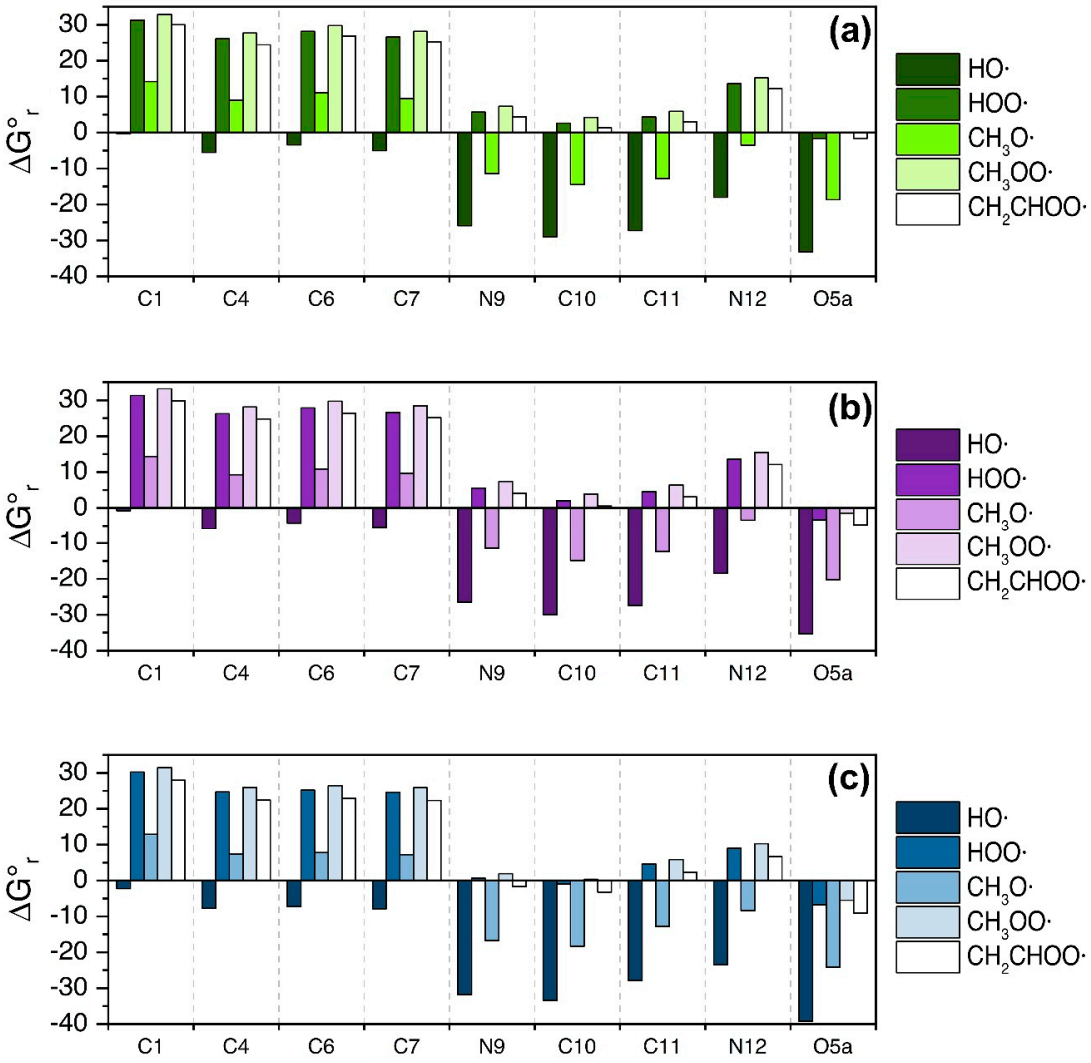

Figure 5. ΔG°_{HAT} (kcal mol^{-1}) in the gas phase (**a**), in water (**b**), and in benzene (**c**) for the scavenging of HO$^{\bullet}$, $CH_3O^{\bullet}$, HOO$^{\bullet}$, $CH_3OO^{\bullet}$, and CH_2=CHOO$^{\bullet}$ through HAT from all the available sites of **2**. Level of theory: (SMD)-M06-2X/6-311+G(d,p)//M06-2X/6-31G (d).

In the gas phase, the largest (negative) ΔG°_{HAT} values are computed for HAT to $HO^{\bullet}$ from sites 9, 10–12, and 5a, with values ranging from −18.02 kcal mol^{-1} (N of the primary amine) to −33.19 kcal mol^{-1} (O). The trend is maintained in the condensed phase, where the reaction energies become more negative with increasing solvent polarity, reaching the values of −23.50 kcal mol^{-1} (N of the primary amine) and −39.23 kcal mol^{-1} (O). Differently from **1** and its metabolites, serotonin also displays some modest activity toward peroxyl radicals, in particular $CH2{=}CHOO^{\bullet}$, when HAT occurs from the O site, with ΔG°_{HAT} going from −1.60 kcal mol^{-1} in the gas phase to −4.75 and −9.05 kcal mol^{-1} in benzene and water, respectively.

The transition states and thus the activation energies were computed only for the exergonic reactions involving the hydroxyl and the methoxyl radical; they are reported in Table 3. In fact, the activation energies for HAT from the most thermodynamically favored site are much higher when considering the other radicals, even when HAT occurs from site 5a (Table S4). By inspecting the values shown in Table 3, in the gas phase and benzene, the activation energies for the amines (sites 9 and 12) are almost identical; conversely, in water, $\Delta G^{\ddagger}_{HAT}$ from the N of the secondary amine becomes almost negligible when the hydroxyl radical is considered, i.e., 0.08 kcal mol^{-1}, a value which, combined with a large negative ΔG°_{HAT}, i.e., −31.84 kcal mol^{-1}, reveals that the HAT from this site is very efficient. Conversely, the thermodynamically most favored process, which is HAT from 5a, has the highest activation energy in water, i.e., 11.23 kcal mol^{-1}.

Table 3. $\Delta G^{\ddagger}_{HAT}$ (kcal mol^{-1}) in the gas phase, benzene, and water, for the scavenging of $HO^{\bullet}$ and $CH_3O^{\bullet}$ through HAT in **2**. Level of theory: (SMD)-M06-2X/6-311+G(d,p)//M06-2X/6-31G(d).

Site	Gas Phase	Benzene	Water	Gas Phase	Benzene	Water
		$HO^{\bullet}$			$CH_3O^{\bullet}$	
9	5.61	6.87	0.08	11.97	14.14	11.12
10	6.86	8.02	7.40	14.43	15.73	14.08
11	6.35	6.91	6.46	12.12	12.92	11.44
12	5.40	6.06	5.14	13.13	14.10	13.10
5a	5.02	6.14	11.23	7.29	8.50	5.36

4. Discussion

The data on HAT thermodynamics and kinetics for fluoxetine and its two metabolites show a selectivity for hydroxyl and alkoxyl radicals, in analogy to what has been reported for melatonin [46]. The most reactive sites are the hydroxyl group and the amine groups. Rather large negative ΔG°_{HAT} values are also computed from the C atoms of the hydrocarbon chain, which is in agreement with the reactivity described for melatonin and zolpidem [38]. In order to verify whether there are more efficient scavenging channels for fluoxetine, we have also investigated the RAF mechanism involving the aromatic C sites. ΔG°_{RAF} values for $HO^{\bullet}$ were computed for **1** as well as for **2**, and are reported in Tables S5 and S6. Focusing on $HO^{\bullet}$, it is worth noticing that the scavenging reactions of **1** that are less exergonic via HAT are significantly more exergonic via RAF, as it emerges for when comparing sites 1, 5, and 13, for which the ΔG°_{HAT} values are −6.14, −3.40, and −5.68 kcal mol^{-1}, and the ΔG°_{RAF} values are −7.98, −9.20, and −8.29 kcal mol^{-1}, respectively. Small negative Gibbs free reaction energies imply a larger stabilization of the reactants than the products. When comparing HAT and RAF, since the reactants are the same, it is useful to inspect the radical product. In Figure 6, the example of the spin densities computed for the radical products obtained from HAT and RAF involving site 1 and $HO^{\bullet}$ is shown. RAF leads to the formation of a radical product in which the spin density is significantly more delocalized on the benzene ring and the adjacent oxygen atom.

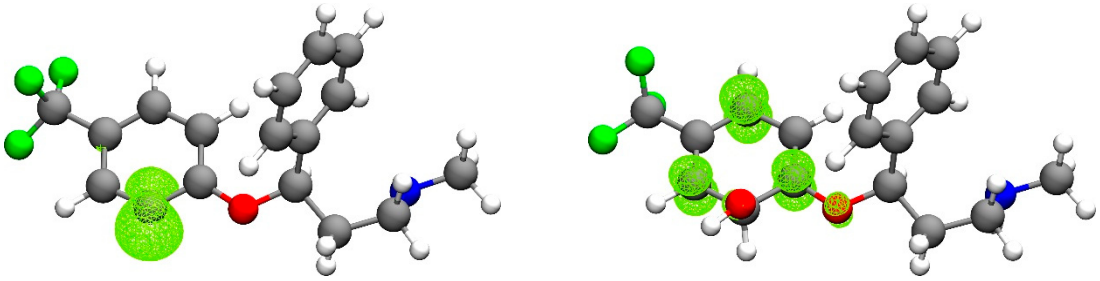

(**a**) (**b**)

Figure 6. Spin densities on (1-H) $^{\bullet}$ when HAT occurs from C1 (**a**) (1OH) $^{\bullet}$ when RAF occurs at C1 (**b**). Level of theory: (SMD)-M06-2X/6-311+G(d,p)//M06-2X/6-31G(d).

There is no clear trend for RAF exergonicity when going from the gas phase to benzene and water. In general, the reactants should be more stabilized with increasing solvent polarity, and so the reaction Gibbs free energies should become more negative from benzene to water. However, this is not observed for sites 5, 6, and 8, which are located in a sterically crowded region of fluoxetine between the two orthogonal phenyl rings. In **2**, both hydroxyl and methoxyl radicals were tested, and we found that in gas-phase serotonin is selective via RAF for HO$^{\bullet}$ except from site 3. The process is weakly exergonic from site 8, too; these sites correspond to the junction carbon atoms. When $CH_3O^{\bullet}$ is considered, the HAT from these sites becomes strongly endergonic. Conversely, exergonic RAF occurs only on sites 1 and 4. The trend in solvent shows that the exergonicity increases with increasing solvent polarity, with the exceptions of sites 2–4 (HO$^{\bullet}$) and 4 ($CH_3O^{\bullet}$).

5. Conclusions

The major outcomes of our analysis can be summarized in the following. (i) Fluoxetine has antioxidant capacity acting as ROS scavenging via the HAT mechanism, and is selective for hydroxyl and methoxyl radicals. (ii) Scavenging may occur also via the RAF mechanism involving the C sites of the benzene rings. (iii) Serotonin is overall a better scavenger of hydroxyl and peroxyl radicals and, thanks to the presence of the alcoholic group, as in **M2**, which is one identified metabolite of fluoxetine, displays antioxidant activity also toward peroxyl radicals. These observations support the hypothesis that the clinical evidence of improvement of oxidative damage associated to fluoxetine therapy is likely due to the enhanced concentration of free serotonin, i.e., is an indirect effect.

Due to the seriousness of depressive disorders and their social implication, strategies to improve clinical symptoms are of considerable importance; particularly, the antioxidant capacity combined with the main therapeutic action of existing drugs is an idea that should be further investigated, and likely screened in silico as well as tested in vitro/vivo.

Supplementary Materials: The following are available online at http://www.mdpi.com/2076-3417/9/17/3631/s1: Tables S1–S6 (Gibbs free reaction and activation energies in the gas phase and solvents of the HAT and RAF processes here described); Cartesian coordinates of all the intermediates and transition states reported in this work.

Author Contributions: Conceptualization, L.O., G.Z. and C.P.; methodology, L.O.; investigation, C.M. and M.D.T.; resources, L.O.; data curation, C.M., M.D.T. and G.R.; writing—original draft preparation, L.O., C.P. and G.R.; writing—review and editing, L.O. and G.Z.; visualization, M.D.T.; supervision, L.O.; funding acquisition, L.O.

Funding: This research was funded by the Università degli Studi di Padova, thanks to the P-DiSC (BIRD2018-UNIPD) project MAD^{3}S (Modeling Antioxidant Drugs: Design and Development of computer-aided molecular Systems); P.I. L.O. All the calculations were carried out on Marconi (CINECA: Casalecchio di Reno, Italy) thanks to the ISCRA Grant REBEL2 (REdox state role in Bio-inspired ELementary reactions 2), P.I.: L.O.; M.D.T. is grateful to Fondazione CARIPARO for financial support (Ph.D. grant).

Conflicts of Interest: The authors declare no conflict of interest.

References

1. Wong, D.T.; Horng, J.S.; Bymaster, F.P.; Hauser, K.L.; Molloy, B.B. A selective inhibitor of serotonin uptake: Lilly 110140, 3-(p-Trifluoromethylphenoxy)-n-methyl-3-phenylpropylamine. *Life Sci.* **1974**, *15*, 471–479. [CrossRef]
2. Wong, D.T.; Perry, K.W.; Bymaster, F.P. The Discovery of Fluoxetine Hydrochloride (Prozac). *Nat. Rev. Drug Discov.* **2005**, *4*, 764–774. [CrossRef] [PubMed]
3. Hiemke, C.; Härtter, S. Pharmacokinetics of selective serotonin reuptake inhibitors. *Pharmacol. Ther.* **2000**, *85*, 11–28. [CrossRef]
4. Fuller, R.W.; Beasley, C.M. Fluoxetine mechanism of action. *J. Am. Acad. Child Adolesc. Psychiatry* **1991**, *30*, 849. [PubMed]
5. Mandrioli, R.; Forti, G.; Raggi, M. Fluoxetine metabolism and pharmacological interactions: The role of cytochrome P450. *Curr. Drug Metab.* **2006**, *7*, 127–133. [CrossRef] [PubMed]
6. Hancu, G.; Cârcu-Dobrin, M.; Budău, M.; Rusu, A. Analytical methodologies for the stereoselective determination of fluoxetine: An overview. *Biomed. Chromatogr.* **2018**, *32*, e4040. [CrossRef] [PubMed]
7. Ni, Y.G.; Miledi, R. Blockage of 5HT2C serotonin receptors by fluoxetine (Prozac). *Proc. Natl. Acad. Sci. USA* **1997**, *94*, 2036–2040. [CrossRef]
8. Wood, A.J.J.; Gram, L.F. Fluoxetine. *N. Engl. J. Med.* **1994**, *331*, 1354–1361. [CrossRef]
9. Zhou, Z.; Zhen, J.; Karpowich, N.K.; Law, C.J.; Reith, M.E.A.; Wang, D.-N. Antidepressant specificity of serotonin transporter suggested by three LeuT–SSRI structures. *Nat. Struct. Mol. Biol.* **2009**, *16*, 652–657. [CrossRef]
10. Spinks, D.; Spinks, G. Serotonin reuptake inhibition: An update on current research strategies. *Curr. Med. Chem.* **2002**, *9*, 799–810. [CrossRef]
11. Ciribassi, J.; Luescher, A.; Pasloske, K.S.; Robertson-Plouch, C.; Zimmerman, A.; Kaloostian-Whittymore, L. Comparative bioavailability of fluoxetine after transdermal and oral administration to healthy cats. *Am. J. Vet. Res.* **2003**, *64*, 994–998. [CrossRef] [PubMed]
12. Caraci, F.; Tascedda, F.; Merlo, S.; Benatti, C.; Spampinato, S.F.; Munafò, A.; Leggio, G.M.; Nicoletti, F.; Brunello, N.; Drago, F.; et al. Fluoxetine prevents Aβ1-42-induced toxicity via a paracrine signaling mediated by transforming-growth-factor-β1. *Front. Pharmacol.* **2016**, *7*, 389. [CrossRef] [PubMed]
13. Black, C.N.; Bot, M.; Scheffer, P.G.; Cuijpers, P.; Penninx, B.W.J.H. Is depression associated with increased oxidative stress? A systematic review and meta-analysis. *Psychoneuroendocrinology* **2015**, *51*, 164–175. [CrossRef] [PubMed]
14. Allen, J.; Romay-Tallon, R.; Brymer, K.J.; Caruncho, H.J.; Kalynchuk, L.E. Mitochondria and mood: Mitochondrial dysfunction as a key player in the manifestation of depression. *Front. Neurosci.* **2018**, *12*, 386. [CrossRef] [PubMed]
15. Novío, S.; Núñez, M.J.; Amigo, G.; Freire-Garabal, M. Effects of fluoxetine on the oxidative status of peripheral blood leucocytes of restraint-stressed mice. *Basic Clin. Pharmacol. Toxicol.* **2011**, *109*, 365–371. [CrossRef] [PubMed]
16. Réus, G.Z.; Matias, B.I.; Maciel, A.L.; Abelaira, H.M.; Ignácio, Z.M.; de Moura, A.B.; Matos, D.; Danielski, L.G.; Petronilho, F.; Carvalho, A.F.; et al. Mechanism of synergistic action on behavior, oxidative stress and inflammation following co-treatment with ketamine and different antidepressant classes. *Pharmacol. Rep.* **2017**, *69*, 1094–1102. [CrossRef] [PubMed]
17. Robertson, O.D.; Coronado, N.G.; Sethi, R.; Berk, M.; Dodd, S. Putative neuroprotective pharmacotherapies to target the staged progression of mental illness. *Early Interv. Psychiatry* **2019**. [CrossRef] [PubMed]
18. Herbet, M.; Gawrońska-Grzywacz, M.; Izdebska, M.; Piątkowska-Chmiel, I. Effect of the interaction between atorvastatin and selective serotonin reuptake inhibitors on the blood redox equilibrium. *Exp. Ther. Med.* **2016**, *12*, 3440–3444. [CrossRef] [PubMed]
19. Caiaffo, V.; Oliveira, B.D.R.; De Sá, F.B.; Evêncio Neto, J. Anti-inflammatory, antiapoptotic, and antioxidant activity of fluoxetine. *Pharmacol. Res. Perspect.* **2016**, *4*, e00231. [CrossRef] [PubMed]
20. Behr, G.A.; Moreira, J.C.F.; Frey, B.N. Preclinical and clinical evidence of antioxidant effects of antidepressant agents: Implications for the pathophysiology of major depressive disorder. *Oxid. Med. Cell. Longev.* **2012**, *2012*, 609421. [CrossRef]

21. Erman, H.; Guner, I.; Yaman, M.O.; Uzun, D.D.; Gelisgen, R.; Aksu, U.; Yelmen, N.; Sahin, G.; Uzun, H. The effects of fluoxetine on circulating oxidative damage parameters in rats exposed to aortic ischemia–reperfusion. *Eur. J. Pharmacol.* **2015**, *749*, 56–61. [CrossRef] [PubMed]
22. Kolla, N.; Wei, Z.; Richardson, J.S.; Li, X.M. Amitriptyline and fluoxetine protect PC12 cells from cell death induced by hydrogen peroxide. *J. Psychiatry Neurosci.* **2005**, *30*, 196–201. [PubMed]
23. Safhi, M.M.; Qumayri, H.M.; Masmali, A.U.M.; Siddiqui, R.; Alam, M.F.; Khan, G.; Anwer, T. Thymoquinone and fluoxetine alleviate depression via attenuating oxidative damage and inflammatory markers in type-2 diabetic rats. *Arch. Physiol. Biochem.* **2019**, *125*, 150–155. [CrossRef] [PubMed]
24. Dalmizrak, O.; Teralı, K.; Asuquo, E.B.; Ogus, I.H.; Ozer, N. The relevance of glutathione reductase inhibition by fluoxetine to human health and disease: Insights derived from a combined kinetic and docking study. *Protein J.* **2019**, 1–10. [CrossRef] [PubMed]
25. Kalogiannis, M.; Delikatny, E.J.; Jeitner, T.M. Serotonin as a putative scavenger of hypohalous acid in the brain. *Biochim. Biophys. Acta Mol. Basis Dis.* **2016**, *1862*, 651–661. [CrossRef] [PubMed]
26. Azouzi, S.; Santuz, H.; Morandat, S.; Pereira, C.; Côté, F.; Hermine, O.; El Kirat, K.; Colin, Y.; Le Van Kim, C.; Etchebest, C.; et al. Antioxidant and membrane binding properties of serotonin protect lipids from oxidation. *Biophys. J.* **2017**, *112*, 1863–1873. [CrossRef] [PubMed]
27. Lobayan, R.M.; Schmit, M.C.P. Conformational and NBO studies of serotonin as a radical scavenger. Changes induced by the OH group. *J. Mol. Graph. Model.* **2018**, *80*, 224–237. [CrossRef] [PubMed]
28. Da Rocha, A.M.; Kist, L.W.; Almeida, E.A.; Silva, D.G.H.; Bonan, C.D.; Altenhofen, S.; Kaufmann, C.G.; Bogo, M.R.; Barros, D.M.; Oliveira, S.; et al. Neurotoxicity in zebrafish exposed to carbon nanotubes: Effects on neurotransmitters levels and antioxidant system. *Comp. Biochem. Physiol. Part C Toxicol. Pharmacol.* **2019**, *218*, 30–35. [CrossRef] [PubMed]
29. Sarikaya, S.B.O.; Gulcin, I. Radical scavenging and antioxidant capacity of serotonin. *Curr. Bioact. Compd.* **2013**, *9*, 143–152. [CrossRef]
30. Orian, L.; Mauri, P.; Roveri, A.; Toppo, S.; Benazzi, L.; Bosello-Travain, V.; De Palma, A.; Maiorino, M.; Miotto, G.; Zaccarin, M.; et al. Selenocysteine oxidation in glutathione peroxidase catalysis: An MS-supported quantum mechanics study. *Free Radic. Biol. Med.* **2015**, *87*, 1–14. [CrossRef] [PubMed]
31. Bortoli, M.; Torsello, M.; Bickelhaupt, F.M.; Orian, L. Role of the Chalcogen (S, Se, Te) in the oxidation mechanism of the glutathione peroxidase active site. *ChemPhysChem* **2017**, *18*, 2990–2998. [CrossRef] [PubMed]
32. Maiorino, M.; Bosello-Travain, V.; Cozza, G.; Miotto, G.; Orian, L.; Roveri, A.; Toppo, S.; Zaccarin, M.; Ursini, F. *Glutathione Peroxidase 4 from Selenium: Its Molecular Biology and Role in Human Health*, 4th ed.; Springer International Publisher: New York, NY, USA, 2016; ISBN 9783319412832.
33. Orian, L.; Toppo, S. Organochalcogen peroxidase mimetics as potential drugs: A long story of a promise still unfulfilled. *Free Radic. Biol. Med.* **2014**, *66*, 65–74. [CrossRef] [PubMed]
34. Wolters, L.P.; Orian, L. Peroxidase activity of organic selenides: Mechanistic insights from quantum chemistry. *Curr. Org. Chem.* **2016**, *20*, 189–197. [CrossRef]
35. Ribaudo, G.; Bellanda, M.; Menegazzo, I.; Wolters, L.P.; Bortoli, M.; Ferrer-Sueta, G.; Zagotto, G.; Orian, L. Mechanistic insight into the oxidation of organic phenylselenides by H_2O_2. *Chem. A Eur. J.* **2017**, *23*, 2405–2422. [CrossRef] [PubMed]
36. Bortoli, M.; Zaccaria, F.; Dalla Tiezza, M.; Bruschi, M.; Fonseca Guerra, C.; Bickelhaupt, F.M.; Orian, L. Oxidation of organic diselenides and ditellurides by H_2O_2 for bioinspired catalyst design. *Phys. Chem. Chem. Phys.* **2018**, *20*, 20874–20885. [CrossRef] [PubMed]
37. Dalla Tiezza, M.; Ribaudo, G.; Orian, L. Organodiselenides: Organic catalysis and drug design learning from glutathione peroxidase. *Curr. Org. Chem.* **2019**. [CrossRef]
38. Bortoli, M.; Dalla Tiezza, M.; Muraro, C.; Pavan, C.; Ribaudo, G.; Rodighiero, A.; Tubaro, C.; Zagotto, G.; Orian, L. Psychiatric disorders and oxidative injury: Antioxidant effects of zolpidem therapy disclosed in silico. *Comput. Struct. Biotechnol. J.* **2019**, *17*, 311–318. [CrossRef] [PubMed]
39. Grimme, S.; Bannwarth, C.; Shushkov, P. A robust and accurate tight-binding quantum chemical method for structures, vibrational frequencies, and noncovalent interactions of large molecular systems parametrized for all spd-block elements (Z = 1–86). *J. Chem. Theory Comput.* **2017**, *13*, 1989–2009. [CrossRef] [PubMed]

40. Bannwarth, C.; Ehlert, S.; Grimme, S. GFN2-xTB—An accurate and broadly parametrized self-consistent tight-binding quantum chemical method with multipole electrostatics and density-dependent dispersion contributions. *J. Chem. Theory Comput.* **2019**, *15*, 1652–1671. [CrossRef] [PubMed]
41. Grimme, S. Exploration of chemical compound, conformer, and reaction space with meta-dynamics simulations based on tight-binding quantum chemical calculations. *J. Chem. Theory Comput.* **2019**, *15*, 2847–2862. [CrossRef] [PubMed]
42. Zhao, Y.; Truhlar, D.G. The M06 suite of density functionals for main group thermochemistry, thermochemical kinetics, noncovalent interactions, excited states, and transition elements: Two new functionals and systematic testing of four M06-class functionals and 12 other function. *Theor. Chem. Acc.* **2008**, *120*, 215–241. [CrossRef]
43. *Gaussian 16*, Revision B.01. Frisch, M.J.; Trucks, G.W.; Schlegel, H.B.; Scuseria, G.E.; Robb, M.A.; Cheeseman, J.R.; Scalmani, G.; Barone, V.; Petersson, G.A.; Nakatsuji, H.; Li, X.; Caricato, M.; Marenich, A.V.; Bloino, J.; Janesko, B.G.; Gomperts, R.; Mennucci, B.; Hratchian, H.P.; Ortiz, J.V.; Izmaylov, A.F.; Sonnenberg, J.L.; Williams; Ding, F.; Lipparini, F.; Egidi, F.; Goings, J.; Peng, B.; Petrone, A.; Henderson, T.; Ranasinghe, D.; Zakrzewski, V.G.; Gao, J.; Rega, N.; Zheng, G.; Liang, W.; Hada, M.; Ehara, M.; Toyota, K.; Fukuda, R.; Hasegawa, J.; Ishida, M.; Nakajima, T.; Honda, Y.; Kitao, O.; Nakai, H.; Vreven, T.; Throssell, K.; Montgomery, J.A., Jr.; Peralta, J.E.; Ogliaro, F.; Bearpark, M.J.; Heyd, J.J.; Brothers, E.N.; Kudin, K.N.; Staroverov, V.N.; Keith, T.A.; Kobayashi, R.; Normand, J.; Raghavachari, K.; Rendell, A.P.; Burant, J.C.; Iyengar, S.S.; Tomasi, J.; Cossi, M.; Millam, J.M.; Klene, M.; Adamo, C.; Cammi, R.; Ochterski, J.W.; Martin, R.L.; Morokuma, K.; Farkas, O.; Foresman, J.B.; Fox, D.J. Gaussian Inc.: Wallingford, CT, USA, 2016.
44. Marenich, A.V.; Cramer, C.J.; Truhlar, D.G. Universal Solvation model based on solute electron density and on a continuum model of the solvent defined by the bulk dielectric constant and atomic surface tensions. *J. Phys. Chem. B* **2009**, *113*, 6378–6396. [CrossRef] [PubMed]
45. Antony, J.; Sure, R.; Grimme, S. Using dispersion-corrected density functional theory to understand supramolecular binding thermodynamics. *Chem. Commun.* **2015**, *51*, 1764–1774. [CrossRef] [PubMed]
46. Galano, A. On the direct scavenging activity of melatonin towards hydroxyl and a series of peroxyl radicals. *Phys. Chem. Chem. Phys.* **2011**, *13*, 7178. [CrossRef] [PubMed]
47. Glendening, E.D.; Landis, C.R.; Weinhold, F. *NBO 6.0*: Natural bond orbital analysis program. *J. Comput. Chem.* **2013**, *34*, 1429–1437. [CrossRef] [PubMed]
48. Lu, T.; Chen, F. Multiwfn: A multifunctional wavefunction analyzer. *J. Comput. Chem.* **2012**, *33*, 580–592. [CrossRef] [PubMed]
49. Bortoli, M.; Wolters, L.P.; Orian, L.; Bickelhaupt, F.M. Addition-elimination or nucleophilic substitution? Understanding the energy profiles for the reaction of chalcogenolates with dichalcogenides. *J. Chem. Theory Comput.* **2016**, *12*, 2752–2761. [CrossRef] [PubMed]
50. Alberto, M.E.; Russo, N.; Grand, A.; Galano, A. A physicochemical examination of the free radical scavenging activity of trolox: Mechanism, kinetics and influence of the environment. *Phys. Chem. Chem. Phys.* **2013**, *15*, 4642. [CrossRef] [PubMed]
51. Galano, A.; Tan, D.X.; Reiter, R.J. Melatonin as a natural ally against oxidative stress: A physicochemical examination. *J. Pineal Res.* **2011**, *51*, 1–16. [CrossRef]
52. Galano, A.; Martínez, A. Capsaicin, a tasty free radical scavenger: Mechanism of action and kinetics. *J. Phys. Chem. B* **2012**, *116*, 1200–1208. [CrossRef]
53. Van Harten, J. Clinical pharmacokinetics of selective serotonin reuptake inhibitors. *Clin. Pharmacokinet.* **1993**, *24*, 203–220. [CrossRef] [PubMed]
54. Strauss, W.L.; Layton, M.E.; Hayes, C.E.; Dager, S.R. 19F magnetic resonance spectroscopy investigation in vivo of acute and steady-state brain fluvoxamine levels in obsessive-compulsive disorder. *Am. J. Psychiatry* **1997**, *154*, 516–522. [PubMed]
55. Benfield, P.; Heel, R.C.; Lewis, S.P. Fluoxetine. *Drugs* **1986**, *32*, 481–508. [CrossRef] [PubMed]
56. Margolis, J.M.; O'Donnell, J.P.; Mankowski, D.C.; Ekins, S.; Obach, R.S. (R)-, (S)-, and Racemic fluoxetine n-demethylation by human cytochrome P450 enzymes. *Drug Metab. Dispos.* **2000**, *28*, 1187–1191. [PubMed]
57. Zarghi, A.; Kebriaeezadeh, A.; Ahmadkhaniha, R.; Akhgari, M.; Rastkari, N. Selective liquid chromatographic method for determination of fluoxetine in plasma. *J. AOAC Int.* **2001**, *84*, 1735–1737. [PubMed]

58. Gupta, R.N.; Steiner, M. Determination of fluoxetine and norfluoxetine in serum by liquid chromatography with fluorescence detection. *J. Liq. Chromatogr.* **1990**, *13*, 3785–3797. [CrossRef]
59. Rohrig, T.P.; Prouty, R.W. A nortriptyline death with unusually high tissue concentrations. *J. Anal. Toxicol.* **1989**, *13*, 303–304. [CrossRef] [PubMed]